Surface & Coatings Technology 232 (2013) 283–289

Contents lists available at ScienceDirect

Surface & Coatings Technology

journal homepage: www.elsevier.com/locate/surfcoat

Non-monotonous evolution of hybrid PVD–PECVD process characteristics on hydrocarbon supply

T. Schmidtová, P. Souček, V. Kudrle, P. Vašina *

Department of Physical Electronics, Kotlářská 2, Masaryk University, 61137 Brno, Czech Republic

ARTICLE INFO

Article history:
Received 25 February 2013
Accepted in revised form 13 May 2013
Available online 21 May 2013

Keywords:
Magnetron sputtering
Diagnostics of deposition process
Nanocomposites
Metal–carbon coatings

ABSTRACT

Hybrid PVD–PECVD process of titanium sputtering in argon and acetylene atmosphere combines aspects of both conventional techniques: sputtering of titanium target (PVD) and acetylene as a source of carbon (PECVD). This process can be used for preparation of metal carbon nanocomposites (MeC/C(:H)) or DLC layers doped with metal (DLC:Me). The aim of this paper is to describe and understand elementary processes influencing the hybrid PVD–PECVD process. A non-monotonous dependence of cathode voltage and current, total pressure and spectral line intensities on acetylene supply flow is reported. Explanation of non-monotonous evolutions through the analysis of the target state correlating the process characteristics with properties of coatings prepared by this process is proposed.

1. Introduction

Hybrid deposition systems combine more than one deposition technique [1]. These techniques are mutually independent and they are being used often in separate deposition chambers [1–4]. An overview of various deposition systems can be found in [2]. The sputtering of a metal target in a mixture of an inert gas and a hydrocarbon gas can be classified as a hybrid process combining PVD and PECVD techniques [5–8]. The source of carbon in the hybrid PVD–PECVD process is dissociated hydrocarbon vapour.

Hybrid PVD–PECVD process is being used for synthesis of metal hydrogenated carbon nanocomposite (MeC/C(:H)) [6,8–13] layers or DLC layers doped with metal (DLC:Me) [14–17]. For example nc-WC/a-C:H [18–21] or nc-TiC/a-C:H [9,22–24] are reported to have good mechanical and tribological properties combining high hardness, good toughness with low friction coefficient and wear which makes these materials industrially attractive for different applications. For the specific case of the titanium target sputtering in hydrocarbon containing atmosphere there exits variety of papers that are focused on the influence of process parameters on properties of deposited coating [8,25–29]. Process features are often omitted.

Hybrid PVD–PECVD process has been previously compared to the conventional reactive magnetron sputtering [30]. Even though the addition of the hydrocarbon is very similar to the adding of oxygen or nitrogen as a reactive gas in reactive sputtering, it was found [30] that hysteresis behaviour typical for reactive magnetron sputtering described by Berg model [31] was completely suppressed during hybrid PVD–PECVD process. Therefore, the hybrid PVD–PECVD depositions do not require complex feedback control. The absence of the hysteresis region was explained [30] by the capability of surfaces to be covered by thick carbon rich layers. In these thick carbon rich layers the carbon can be bound mutually in contrary to metal oxides/nitrides formation on surfaces during classical reactive magnetron sputtering where oxygen/nitrogen can be bound only to the metal. Nevertheless the target covering by these carbon rich layers during the hybrid PVD–PECVD process is still similar to the target poisoning by a reactive gas because it prevents the sputtering of the metal. So for description of both processes the phrases 'target poisoning' and 'target cleaning' can be understood and used.

The aim of this paper is to describe and understand elementary processes influencing the hybrid PVD–PECVD process governing the properties of the deposited coatings. We report a non-monotonous dependence of cathode voltage and current, total pressure and spectral line intensities on acetylene supply flow. We report on the dependence of the chemical composition and mechanical properties of the coatings on the acetylene flow. We provide an explanation of non-monotonous dependences through the analysis of the target state. The role of RF bias on the substrate and magnetron DC power on the process characteristics is also discussed.

2. Experimental configuration

Experimental measurements were done on semi-industrial magnetron sputtering system Alcatel SCM 650. Experimental setup drawing is shown in Fig. 1. A titanium target (purity 99.99%) 20 cm in diameter was mounted on a well balanced magnetron head, sputtering-up geometry was used. The magnetron plasma was well localized near the target, it does not extent to the substrate. The target-to-substrate distance was 7 cm. The chamber was pumped by turbomolecular pump

* Corresponding author: Tel.: +420 549 496 479.
E-mail address: vasina@physics.muni.cz (P. Vašina).

0257-8972/$ – see front matter © 2013 Elsevier B.V. All rights reserved.
http://dx.doi.org/10.1016/j.surfcoat.2013.05.014

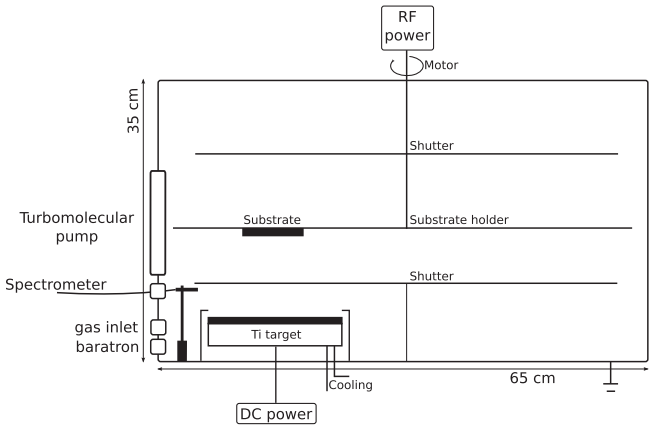

Fig. 1. Drawing of the experimental setup.

(700 l s^{-1}) backed by Roots pump. The base pressure was typically 10^{-4} Pa. During the deposition the pump was throttled to the pumping speed of 40 l s^{-1}. The argon (purity 99.999%) flow was kept constant at 20 sccm for all experiments. The typical working pressure was around 1 Pa.

For the study of the hybrid PVD–PECVD process acetylene (purity 99.6%) was used as carbon source. The acetylene flow ranged from 0 to 16 sccm. Magnetized plasma was ignited by DC power (1 kW or 2 kW) combined with or without RF substrate bias (225 W ~ −100 V). To enable comparison of the deposition process and deposited coating properties, the values of DC power, RF bias and supply flows of Ar and C_2H_2 were selected to correspond to values used in paper [23,24] where properties of deposited n-TiC/a-C:H coatings were studied in details. The DC generator was operated in constant power mode. Prior to each experiment, the target was thoroughly cleaned both mechanically and by Ar bombardment until the discharge voltage typical for pure Ti target was reached.

Spectrometer Avantes SD2000 was used as a diagnostic tool. Atomic spectral lines of titanium at 365 nm, argon at 420 nm and hydrogen at 656 nm were chosen for the study. There were no lines attributed to carbon or other fragments of acetylene in observed spectral range of 250–670 nm. Discharge parameters used for electrical diagnostics were the target voltage and the discharge current. The total pressure in the vacuum chamber was also recorded using MKS Baratron.

The depositions were carried out for 45 min at constant acetylene flow on high speed steel (HSS) and cermet tungsten carbide (WC) substrates. The DC power to the magnetron was set at the desired value and the substrate bias was −100 V. Chemical composition of the coatings was determined by Rutherford backscattering (RBS) and elastic recoil detection analysis (ERDA) methods using a Van de Graaff generator and TANDETRON with linear electrostatic accelerators. Fischerscope H100 depth sensing indenter equipped with a Berkovich tip was used to study the indentation response of the coating samples. The hardness and the indentation modulus were evaluated using the standard procedure proposed by Oliver and Pharr [32]. The EDX measurements were performed on JEOL JSM 6460 with Inca Energy EDX detector at 20 kV acceleration voltage.

For the study of the target state the following experimental settings were used. The depositions for various C_2H_2 flows were performed at conditions described in [23,24]. Target photo-documentation was done after each opening of the vacuum chamber. In order to quantify the target state on the evolution on the acetylene supply the pixel counting for target areas of interest were done for each taken photograph. The pixel counting determined the relative amount of studied parts. The pixel count was done at the racetrack part only, because the racetrack, the target erosion zone, plays the key role for the magnetron discharge. For the EDX (Energy-dispersive X-ray spectroscopy) study of the target racetrack coverage by Ti–C phases, Ti square samples (1 cm × 1 cm) were used and placed on the racetrack zone. One edge of Ti sample was placed in the racetrack centre and the other at the racetrack outer edge.

3. Results and discussion

3.1. Process characteristics

Typical overall hybrid PVD–PECVD process characteristics are given in Fig. 2. There are shown the dependences of cathode voltage and discharge current together with total pressure and spectral emission line intensities on the acetylene supply flow for 2 kW DC power applied on the magnetron target with −100 V RF bias.

Before measurement of each point, the target was thoroughly cleaned by Ar bombardment without the presence of acetylene to ensure the same target conditions and to eliminate the influence of previous measurements. The cleaning of the target covered by thick carbon rich layers takes long time [30]. The steady-state conditions of the hybrid PVD–PECVD process are reached in order of tens of minutes after acetylene injection. In Fig. 2 the full black square points denote the measured values with increasing acetylene flows — on the way from the clean target. When measuring with the decreasing acetylene flows, the cleaned target was exposed for 3 min to 30 sccm of C_2H_2 for full poisoning. The Fig. 2 the hollow red circle points denote measured values with decreasing acetylene flows — on the way from the poisoned target.

Fig. 2 demonstrates that the hybrid PVD–PECVD process does not exhibit hysteresis behaviour. The electrical characteristics in Fig. 2(a) and (b) are non-monotonous; a certain local minimum in voltage and local maximum in discharge current evolutions is observed. The discharge voltage and current are increasing and decreasing respectively while the DC generator was operated in constant power mode meaning that the current and voltage dependencies are inverted. There is also no rapid evolution of total pressure in the chamber with acetylene flow, see Fig. 2(c). The pressure is increasing with increasing acetylene flow almost linearly.

Dependence on acetylene supply flow of hydrogen, titanium and argon emission lines given by optical emission spectra are shown in Fig. 2(d)–(f). In Fig. 2(d) the non-monotonous evolution of hydrogen alpha line is plotted. It is increasing rapidly with increasing acetylene flow but for higher flows it is sharply decreasing, a maximum of hydrogen line intensity is observed for certain acetylene supply flow. The evolution of titanium emission line in Fig. 2(e) is different, it is almost linear. Looking at the argon emission line, see Fig. 2(f), its intensity is slightly decreasing, increasing and then decreasing as acetylene flow increases.

From the general overview of presented data, one can conclude that there exist three distinctive zones in which studied parameters evolve in a characteristic way. For 2 kW DC power applied on the magnetron target there is zone I from 0 to approximately 6 sccm of C_2H_2, zone II approximately from 6 to 12 sccm of C_2H_2 and zone III for higher flows than 12 sccm of C_2H_2.

The zone I is characterized by the increasing discharge voltage, pressure and hydrogen emission intensity and by the increase in discharge current, titanium emission intensity and slight decrease in argon emission. The zone II is characterized by the increase in discharge current, pressure, hydrogen emission intensity and slight increase in argon emission together with decreasing discharge voltage and titanium emission. In the zone III again the increase in the target voltage together with the slight increase in the total pressure can be observed, the decreasing values of the discharge current, titanium, hydrogen and argon is characteristic. Summarizing overview of each parameter evolutions within three defined zones is given in Table 1.

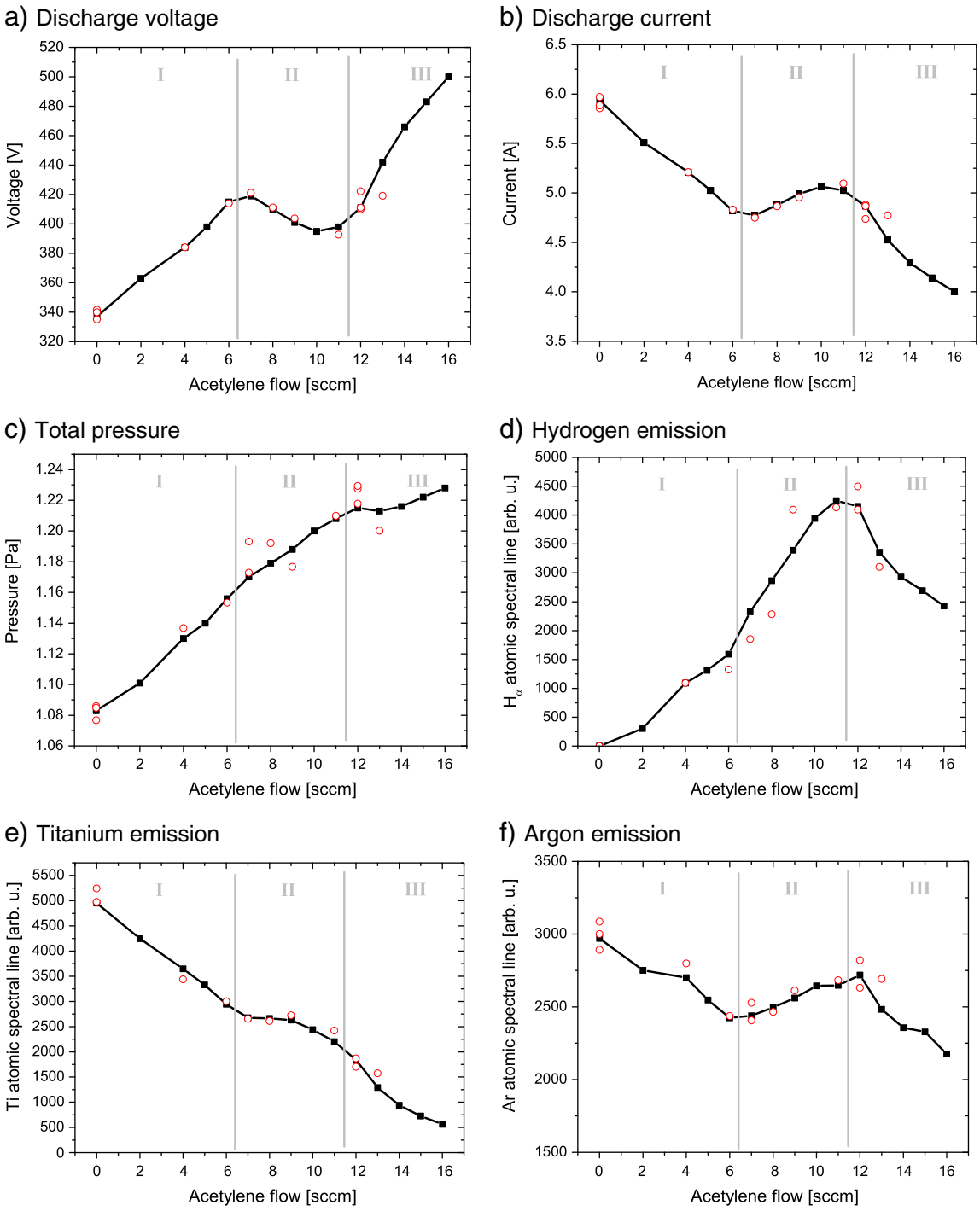

Fig. 2. Dependences of discharge voltage, discharge current, total pressure and spectral emission lines on acetylene flow. Black full square points are values obtained with increasing acetylene flow – on the way from clean target and red hollow circular points are values obtained with decreasing acetylene flow – on the way from poisoned target.

Table 1
Summarizing overview of each parameter evolutions within zones I–III.

	Voltage (current)	Spectral intensity			Relative density		
		H	Ti	Ar	H	Ti	Ar
Zone I	↗ (↘)	↗	↘	↘	↗	↗	→
Zone II	↘ (↗)	↗	↗	↗	↗	↘	→
Zone III	↗ (↘)	↘	↘	↘	→	↗	→

3.2. Film properties

A set of coatings was prepared using this hybrid PVD–PECVD process at acetylene flows of 8–14 sccm (i.e. in zones II and III) and analysed [24]. The chemical composition of the coatings behaves more monotonously as can be seen in Fig. 3. Titanium content decreases while carbon content increases with higher acetylene flow. Hydrogen content remains stable <10% and also the oxygen contamination remains low for the whole deposition range. The stoichiometric composition where

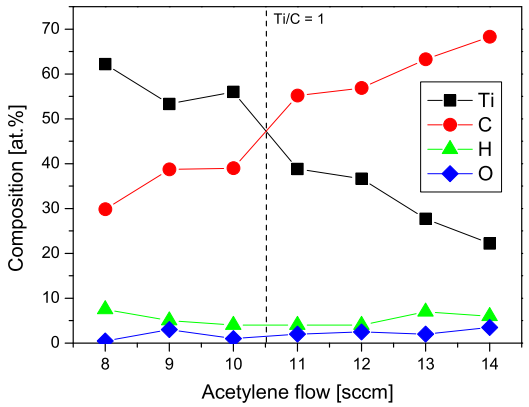

Fig. 3. Chemical composition of nc-TiC/a-C:H coatings depending on acetylene flow during deposition.

Ti/C = 1 was achieved for acetylene flow of ~10.5 sccm, which belongs to aforementioned zone II.

The mechanical properties show a distinct peak at acetylene flow of 12 sccm (see Fig. 4). At this point the hardness reaches 46 ± 2 GPa and Young's modulus 414 ± 7 GPa. The mechanical properties decrease with both lower and higher acetylene flows. The flow of 12 sccm lies on the border between zones II and III.

More detailed study of the properties of the thin films deposited by the hybrid PVD–PECVD process including evolution of the deposition rate, residual stress, microstructure, etc. with acetylene supply was presented in the associated paper [24].

3.3. The state of the target

For reactive magnetron sputtering, it was reported that the electrical characteristics are related to the state of the target; the target poisoning by a compound of different coefficient of secondary electron emission from the original target material results in a change in the target voltage [33]. In classical reactive magnetron sputtering the cathode voltage decreases/increases monotonously with the partial pressure of the reactive gas as there is a monotonous and continuous coverage of the target surface by a compound. However the electrical characteristics in Fig. 2(a) and (b) have distinctive evolution on the acetylene flow. A characteristic local minimum (maximum) in voltage (current) evolution is observed. As the pressure is evolving in Fig. 2(c) only a little its influence on the electrical characteristics should be negligible and the presence of the local minimum (maximum) should be related to the evolution of the state of the target in a different way during hybrid PVD–PECVD process than during classical reactive magnetron sputtering.

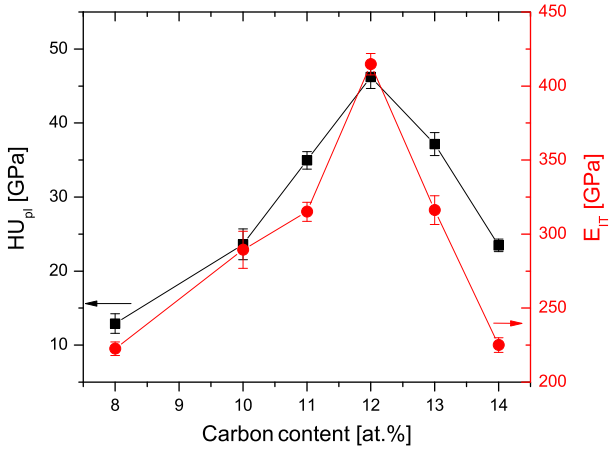

Fig. 4. Mechanical properties of nc-TiC/a-C:H coatings depending on acetylene flow during deposition.

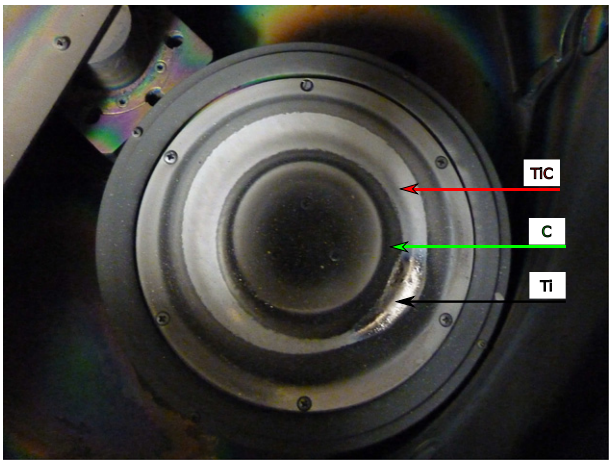

Fig. 5. Photograph of the target after sputtering by 2 kW DC power with RF substrate bias −100 V for 12 sccm of acetylene at steady-state conditions. Along the racetrack region three differently 'coloured' regions are visible. The pure metallic region is denoted as Ti, the grey as TiC and black as a-C.

For hybrid PVD–PECVD process a target surface photography is shown in Fig. 5. The target was covered by three differently 'coloured' regions. The following can be distinguished: a metallic region, a black region, and a grey region. The metallic region is of the same colour as the original titanium target, so it is denoted as titanium (Ti). The black layer which was easily removable by hand or an abrasive resembles the soots and so it is denoted as carbon (C). The grey region which is matt, compact and very difficult to remove by an abrasive is a transition between the metallic and black regions. It is similarly coloured to titanium carbide so this region is denoted as titanium carbide (TiC).

It was of interest to see the target surface changes after sputtering in the same conditions for various acetylene flows. In Fig. 6 are shown photographs of three target halves for selected 3, 9 and 13 sccm of acetylene flows. For better visualization the target racetrack is delimited by red highlights. For 3 sccm of C_2H_2 the target racetrack was mostly Ti, for 9 sccm of C_2H_2 the target was mainly grey — mainly TiC and for 13 sccm of C_2H_2 the racetrack was carbon rich with black and grey regions. Clearly some evolution of the target state with the acetylene flow is visible.

Calculation of the relative target racetrack coverage by Ti, TiC and C parts as was done by the pixel counts as described in the experimental section. In Fig. 7 shown are racetrack coverage percentages

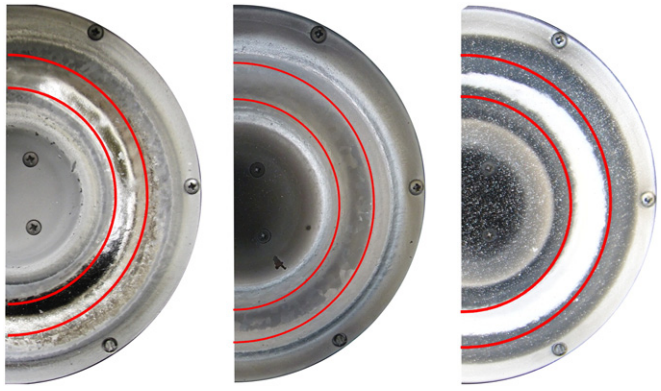

Fig. 6. Photographs of three selected target halves for 3, 9 and 13 sccm of acetylene after achievement of steady-state conditions during deposition. The target racetrack region is highlighted.

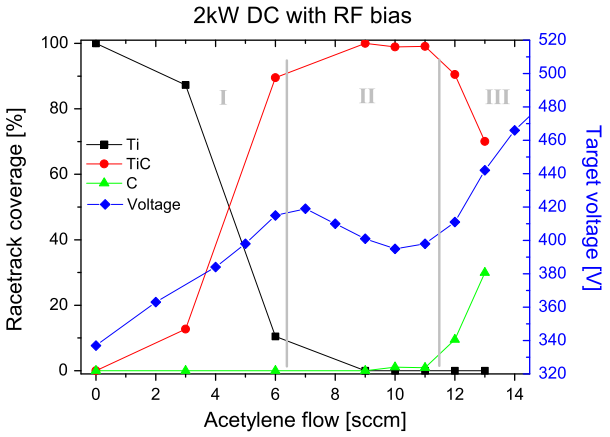

Fig. 7. Racetrack coverage by Ti, TiC and C on acetylene supply. Voltage characteristics with three zones behaviour is correlated with plotted racetrack coverage.

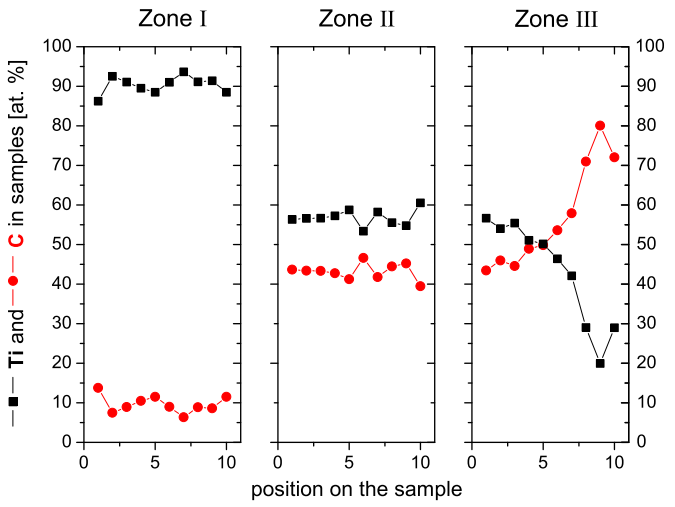

Fig. 8. EDX analysis of three Ti square samples (1 cm × 1 cm) placed in the target racetrack during the deposition at different acetylene flows. Position 0 marks the racetrack centre, position 11 marks the racetrack outer edge.

for the three studied parts and the results are also correlated with the three zone behaviour of voltage characteristics.

In the zone I from 0 to approximately 6 sccm of C_2H_2 Ti regions are diminishing on behalf of TiC regions, the racetrack is titanium rich. In the zone II approximately from 6 to 12 sccm of C_2H_2 the racetrack is composed mainly by TiC region. For higher flows of C_2H_2 in the zone III the TiC parts are overtaken by C, the racetrack becomes carbon rich. Combining information from discharge voltage characteristics with the racetrack coverage we can conclude that the voltage increase in the zone I is connected with the creation of TiC on the target racetrack. In the zone II, the voltage slightly decreases with acetylene inflow (by about 5%) and the voltage local minimum is observed at 11 sccm of acetylene supply. In the zone II, mainly the presence of the grey colour TiC was detected in the racetrack region (see Fig. 7) leading us to a conclusion that the voltage decrease should be related with the evolution of TiC Invoking the phase diagram of Ti–C [34,35], we suppose the voltage decrease to be caused by the evolution of the TiC stoichiometry in the racetrack region from the substoichiometric TiC (at 6 sccm of C_2H_2) to stoichiometric TiC (around 11 sccm of C_2H_2). The rapid voltage increase with higher acetylene flows in the zone III is clearly related to the carbon formation in the racetrack. Its composition is therefore carbon rich TiC/C. Therefore increasing of the acetylene supply flow results in continuous phase change from Ti-rich Ti/TiC (zone I) to mainly single phase TiC (zone II) and finally to carbon-rich TiC/C(zone III). The evolution of the target state is similar to phase changes in the growing TiC/C films with increase carbon content as can be found for example in [10,35].

For the better understanding of the racetrack coverage by Ti–C phases the analysis was performed on the Ti square samples placed on the cathode surface. The results for the three studied zones of acetylene flows are shown in Fig. 8. Note that the EDX method gathers the information from approximately 1 C_2H_2 volume of the top layer of the analysed material. As the thickness of the target layer which has been modified by the process is unknown and probably varies with acetylene supplies, only qualitative information of Ti and C compositions can be derived. From Fig. 8 the racetrack homogeneity is clearly observed. For low acetylene flows in the zone I the Ti/C ratio is very high and approaching the zone II the Ti and C abundances become equal. In the zone III where the amorphous carbon enters the racetrack region a clear evolution of composition is seen from racetrack centre to its edge where Ti/C ratio is reversed.

In our case, the maximal hardness of 46 ± 2 GPa and indentation modulus of 415 ± 7 GPa were measured for coatings with 55 at.% C deposited at the conditions close to the frontiers between zones II and III, where the target surface is covered by stoichiometric TiC. According to the generic design concept [36,37], this high hardness is based on the combination of the absence of dislocation activity in the small TiC nanocrystals and blocking of a-C:H grain boundary sliding by the formation of a strong interface between the two phases. Thus, the coatings with maximal hardness should show certain excess of carbon over titanium to form nanocomposite structure. In hybrid PVD–PECVD process, both the target and the substrate are being exposed to the flux of carbonaceous species originating from acetylene dissociations. Simultaneously to target poisoning, the target is being sputter cleaned providing additional flux of carbon atoms on the substrate. Similarly to reactive magnetron sputtering [31], higher relative amount of carbon could be expected to be found in the growing film than at the target surface which has been experimentally proved for sputtering of Ti in mixture of Ar and CH_4 [25]. In our experimental configuration, deposition process at conditions between zones II and III caused the optimal conditions for the growth of the nc-TiC/a-C:H with the maximal hardness. Depending on the experimental conditions, such as the magnetron head design and position of argon and acetylene gas inlet, the conditions to deposit coatings with maximal hardness could be slightly shifted, however they should be expected to be located always close to the frontiers between the zones II and III, where the target is covered by TiC and coating composition is slightly overstoichiometric with respect to carbon.

3.4. Relative evolution of concentrations of Ar, H and Ti in plasma

Assuming direct excitation of a ground state particle by an electron impact, the intensity of a spectral line depends on the concentration of electrons in the plasma bulk, concentration of ground state particles and excitation rate which is a factor proportional to overlap of excitation cross section and electron energy distribution function (EEDF). The flux of ions to the sheath edge is proportional to the ion density (which is equal to the electron density in the plasma) times the ion acoustic velocity, typically with a factor of 0.6 according to Bohm presheath diffusion criterion [38]. The ions are then accelerated by the sheath potential and bombard the cathode/target surface causing secondary electron emission and sputtering. Thus, the evolution of the concentration of electrons in the plasma is reflected by the discharge current. Assuming that electron energy distribution function, i.e. excitation rate and ion acoustic velocity does not depend on C_2H_2 supply, ratio of the atomic line intensities and discharge current provides the evolution of the ground state particle densities in plasma.

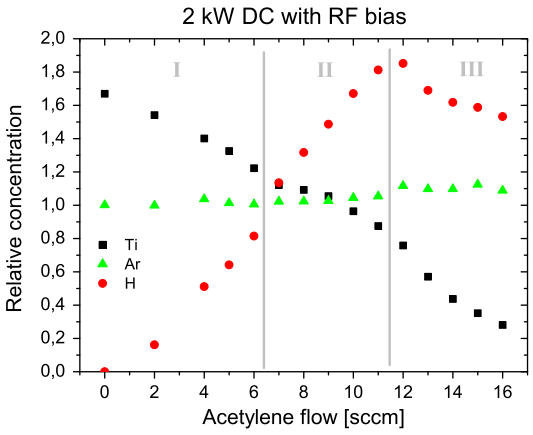

Fig. 9. Dependence of the relative concentrations of Ti, Ar and H in plasma on acetylene supply.

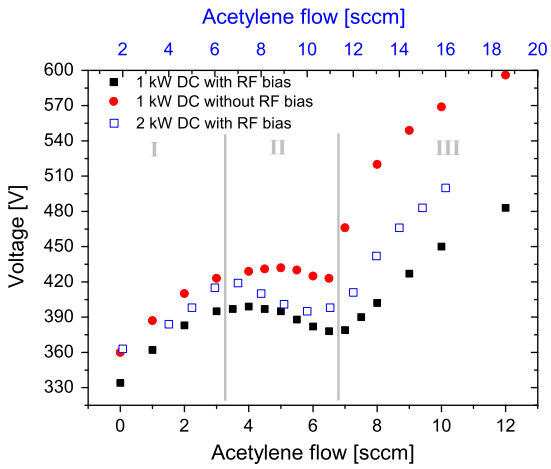

Fig. 10. Voltage characteristics on the acetylene supply flow for 1 kW DC with and without applied RF bias (225 W ~ −100 V).

The evolution of the relative concentrations of Ar, H and Ti in plasma volume is plotted in Fig. 9 together with marked zones I, II and III. The comparison of evolutions of the relative concentrations with other process parameters can be found in Table 1. Despite that the Ar line intensity evolves with C_2H_2 flow the calculated Ar concentrations are constant for all zones supporting the hypotheses on EEDF and ion acoustic velocity to be independent on C_2H_2 supply. Decrease of Ar line intensity in zone I, increase in zone II and decrease in zone III that follow the evolution of the discharge current perfectly (compare Fig. 2(b) and (f)) is caused by evolution of the plasma density and not by the evolution of the buffer gas concentration with the acetylene supply. The titanium concentration is decreasing almost linearly though all zones showing that by increasing the C_2H_2 flow the amount of sputtering Ti is decreasing linearly without any rapid transition.

The hydrogen concentration is increasing in zones I and II and despite that the well pronounced maximum of hydrogen line intensity was observed at the frontiers between the zones II and III, in the zone III the hydrogen concentration is not increasing anymore but it stays rather independent on C_2H_2 supply. The decrease of hydrogen emission in the zone III (see Fig. 2(d)) is not caused by decrease of hydrogen atom concentration (see Fig. 9) but should be related to the steep decrease of discharge current (i.e. plasma density) linked with a steep increase in the discharge voltage to maintain the discharge (see Fig. 2(a)) while the generator was operating in the constant power mode. For high amount of acetylene in the volume it is difficult to estimate the extent of the volume reactions of acetylene fragments. The constant hydrogen atom density in the zone III could be caused by two opposite effects that act simultaneously — an increase of acetylene supply is followed by the reduced ability of the plasma to dissociate acetylene molecules and produce hydrogen atoms due to lower plasma density (lower discharge current, higher voltage to sustain plasma). It is therefore possible that the production of atomic hydrogen is constant or even decreasing with the acetylene supply in the zone III. Other possible explanation for constant hydrogen atom concentration with acetylene supply could be that the substrate film is growing with high content of carbon matrix where significant amount hydrogen could be stored. However the film analysis in the acetylene in the range between 9 and 14 sccm showed, that the hydrogen content in the films is constant around 5% [23,24].

3.5. Influence of magnetron power and substrate bias

The effect of DC power applied on the magnetron target on the hybrid PVD–PECVD process evolution on acetylene supply was studied. By lowering the applied DC power from 2 kW to 1 kW the general trends (three zones behaviour) observed at electrical characteristics Fig. 2(a), (b) and Fig. 7 are preserved, see Fig. 10. The three zones are only shifted towards lower acetylene flows, as applying half power on the magnetron target shifts the boundaries of three zones roughly to half the acetylene flows.

The effect of applying RF bias to the substrate can also be seen in Fig. 10. Substrate bias of −100 V was set by 225 W RF power which was a quarter of the 1 kW DC power applied on the magnetron target. Such relatively high RF power applied on the substrate could be influencing the evolution of hybrid PVD–PECVD process on acetylene supply. Fig. 10 demonstrates that the three zones of the target state and entire process characteristics are not shifted with respect to C_2H_2 flow providing only negligible influence of RF plasma near the substrate on the evolution of the trends of deposition process characteristics.

4. Conclusions

The hybrid PVD–PECVD process of titanium sputtering in argon and acetylene atmosphere does not show the hysteresis behaviour. The absence of hysteresis region avoids process stability problems met in conventional reactive magnetron sputtering making the hybrid PVD–PECVD process relatively easy to control. Three distinctive zones were identified in the process evolution with the acetylene supply.

For the low range of acetylene flows (zone I) the voltage is increasing due to TiC formation on the surface of the target racetrack at the expense of Ti and the relative concentration of Ti in plasma is decreasing while the H concentration is increasing due to acetylene fragmentation in plasma volume. For medium range of acetylene flows (zone II) the target voltage stops increasing or it is slightly decreased. The racetrack is covered mainly by TiC. Ti concentration in plasma phase is still decreasing and hydrogen concentration continues to increase. Stoichiometric TiC coatings are being deposited at this zone. For high acetylene flows (zone III) the target voltage is rapidly increasing, the carbon layers start to penetrate into the target racetrack and the composition of the racetrack surface becomes carbon rich. The Ti concentration in plasma phase is still decreasing but H concentration is not evolving further, it remains more or less constant. On the border of zones II and III the nc-TiC/a-C:H coatings with highest hardness and Young's modulus were prepared. For the studied range of acetylene supply the Ar concentration remains the same.

Reduction of the power applied on the target keeps the three zone behaviour of the process. It shifts zone boundaries towards lower acetylene flows. Halving the magnetron power shifts the boundaries to half of the acetylene flows. RF bias does not significantly influence

the hybrid PVD–PECVD process characteristics. By varying the RF bias for constant magnetron power desired self-bias on the substrate can be set without modifying the overall process behaviour.

Acknowledgement

This research has been supported by Czech Science Foundation contract 104/09/H080 and 205/12/0407 and R&D centre for low-cost plasma and nanotechnology surface modifications CZ.1.05/2.1.00/03.0086 funded by European Regional Development Fund. Pavel Souek acknowledges the Brno City Municipality as holder of Brno PhD Talent Financial Aid. The authors would like to acknowledge Dr. V. Peřina from the Nuclear Physics Institute of the ASCR for RBS measurements and Dr. J. Buršík from the Institute of Physics of Materials of the ASCR for EDX measurements.

References

[1] D.M. Mattox, The Foundations of Vaccum Coating Technology, William Andrew Publishing, 2003. , (ISBN 1-800-932-7045).
[2] J.P. Celis, D. Drees, M.Z. Huq, P.Q. Wu, M. De Bonte, Surf. Coat. Technol. 113 (1999) 165.
[3] A. Matthews, A. Leyland, Surf. Coat. Technol. 71 (1995) 88.
[4] A. Daniel, T. Duguet, T. Belmonte, Appl. Surf. Sci. 253 (2007) 9323.
[5] J.T. Harnack, F. Thieme, C. Benndorf, Surf. Coat. Technol. 39 (40) (1989) 285.
[6] J.T. Harnack, C. Benndorf, Mater. Sci. Eng. A140 (1991) 764.
[7] C. Benndorf, T.J. Harnack, U. Fell, Surf. Coat. Technol. 48 (1993) 345.
[8] P.Y. Tessier, R. Issaoui, E. Luias, M. Boujtita, A. Granier, B. Angleraud, Solid State Sci. 11 (2009) 1824.
[9] Y.T. Pei, D. Galvan, J.Th.M. De Hosson, A. Cavaleiro, Surf. Coat. Technol. 198 (2005) 44.
[10] W. Gulbinski, S. Mathus, H. Shen, T. Suszko, A. Gilewicz, B. Warcholinski, Appl. Surf. Sci. 239 (2005) 302.
[11] W. Kulisch, P. Colpo, F. Rossi, D.V. Shtansky, E.A. Levashov, Surf. Coat. Technol. 118–119 (2004) 714.
[12] T. Ghodselahi, M.A. Vesaghi, A. Shafiekhani, A. Baradaran, A. Karimi, Z. Mobini, Surf. Sci. Technol. 202 (2008) 2731.
[13] J. Bruckner, T. Mantyla, Surf. Coat. Technol. 59 (1993) 166.
[14] C. Donnet, Surf. Coat. Technol. 100–101 (1998) 180.
[15] B. Oral, K.-H. Ernst, C.J. Schmutz, Diamond Relat. Mater. 5 (1996) 932.
[16] N. Yao, A.G. Evans, C.V. Cooper, Surf. Coat. Technol. 179 (2004) 306.
[17] G. Ma, S. Gong, G. Lin, L. Zhang, G. Sun, Appl. Surf. Sci. 258 (2012) 3045.
[18] S. Zhou, L. Wang, S.C. Xang, Q. Xue, Appl. Surf. Sci. 257 (2011) 6971.
[19] S.J. Park, K.-R. Lee, D.-H. Ko, K.Y. Eun, Diamond Relat. Mater. 11 (2002) 1747.
[20] A. Czyzniewski, Thin Solid Films 433 (2003) 180.
[21] C. Rebholtz, J.M. Schneider, H. Ziegele, B. Rahle, A. Leyland, A. Matthews, Vacuum 49 (1998) 265.
[22] Y. Wang, X. Zhang, X. Wu, H. Zhang, X. Zhang, Appl. Surf. Sci. 254 (2008) 5085.
[23] P. Vasina, P. Soucek, T. Schmidtova, M. Elias, V. Bursikova, M. Jilek, M. Jilek Jr., J. Schafer, J. Bursik, Surf. Sci. Technol. 205 (2011) S53.
[24] P. Soucek, T. Schmidtova, L. Zabransky, V. Bursikova, P. Vasina, O. Caha, M. Jilek, A. El Mel, P.Y. Tessier, J. Schafer, J. Bursik, V. Perina, R. Miksova, Surf. Coat. Technol. 211 (2012) 111.
[25] J.-E. Sundgren, B.-O. Johansson, S.-E. Karlsson, Thin Solid Films 105 (1983) 353.
[26] J.-E. Sundgren, B.-O. Johansson, S.-E. Karlsson, H.T.G. Hentzell, Thin Solid Films 105 (1983) 367.
[27] J.-E. Sundgren, B.-O. Johansson, H.T.G. Hentzell, S.-E. Karlsson, Thin Solid Films 105 (1983) 385.
[28] O.A. Fouad, A.K. Rumaiz, S.I. Shah, Thin solid Films 517 (2009) 5689.
[29] V.Yu. Kulikovsky, F. Fendrych, L. Jastrabik, D. Chvostova, Surf. Coat. Technol. 91 (1997) 122.
[30] T. Schmidtova, P. Soucek, P. Vasina, J. Schafer, Surf. Coat. Technol. 205 (2011) S299.
[31] S. Berg, T. Nyberg, Thin Solid Films 476 (2005) 215.
[32] W.C. Oliver, G.M. Pharr, J. Mater. Res. 19 (2004) 3.
[33] D. Depla, G. Buyle, J. Haemer, R. DeGryse, Surf. Coat. Technol. 200 (2006) 4329.
[34] K. Frisk, Calphad 27 (2003) 367.
[35] D.A. Andersson, P.A. Korzhavyi, B. Johansson, Calphad 32 (2008) 543.
[36] S. Veprek, S. Reiprich, Thin Solid Films 268 (1995) 64.
[37] S. Veprek, J. Vac. Sci. Technol. A 17 (1999) 2401.
[38] D. Bohm, in: A. Guthrie, R.K. Wakerling (Eds.), McGraw-Hill, New York, 1949, p. 77.